THE INFLUENCE OF A RADIAL WAKE VARIATION OVER THE PROPELLER DISC ON THE RELATIVE ROTATIVE EFFICIENCY ;

- A THESIS -

By: Hugo Mach.

Submitted in partial fullfilment of the Requirements for the BACHELOR OF SCIENCE DEGREE from the Massachusetts Institute of Technology, Department of Naval Architecture and Marine Engineering.

Signature of Author _____

Hugo Mach.

May, 1947.

Cambridge, Massachusetts,

May 20th, 1947.

Professor Joseph L. Newell,
Secretary of the Faculty,
Massachusetts Institute of
Technology,
Cambridge, 39, Massachusetts.

Dear Sir,

In accordance with the requirements for the Degree of Bachelor of Science, I herewith submit this Thesis entitled "The Influence of a Radial Wake Variation Over the Propeller Disc on the Relative Rotative Efficiency".

Respectfully submitted,

HUGO MACH.

- TABLE OF CONTENTS -

Table of Contents (Continued) Page.

- FORMULAS AND CONSTANTS -

1. $J = \frac{V}{n \times d} = \frac{60 \times V}{R \times d}$ (Dimensionless)

U N I T S

V feet/sec

n = $\frac{RPM}{60}$ = RPS

d = Diameter in feet.

R = RPM

---

2. Velocity: V = (Range Constant) $\times \sqrt{\mu \times H(ft/sec)}$

μ = Temperature Correction Factor for Velocity Cage.

Range Constant: See Plot

H = m/m Bromo-benzine.

---

3. Thrust Coefficient K_t:

$$K_t = \frac{T_{corr}}{\rho \times n^2 \times d^4} = \frac{T_{corr} \times 3600}{\rho \times R^2 \times d^4} \text{ (dimensionless)}$$

Tcorr = Thrust corrected for hub diameter in lbs(see Plot)

ρ = Density.

Formulas and Constants (Continued)

U N I T S.

4. Torque Coefficient K_q:

$$K_q = \frac{Q_{corr} \times 0.8928}{\rho \times n^2 \times d^5} = \frac{Q_{corr} \times 0.8928 \times 3600}{\rho \times R^2 \times d^5}$$

(dimensionless) Q_{corr}=Torque corrected for Gage error in degrees.

---

5. Efficiency. e :

$$e = \frac{V \times T_{corr}}{2 \times \pi \times n \times Q_{corr}} = \frac{30 \times V \times T_{corr}}{2\pi \times Q_{corr} \times R} =$$

$$= \frac{J \times K_t}{2\pi \times K_q} = 0.1593 \frac{JK_t}{Kq.} \quad \text{(Dimensionless)}$$

---

6. Cavitation Constant σ_n:

$$\sigma_n = \frac{P - P_v}{\times n^2 \times d^2} \quad \text{(dimensionless)}$$

$$(P - P_v)\ \text{m/m Hg} = \frac{(P - P_v)\#/ft^2}{2.7743}$$

P=Absolute Pressure

P_v=Vapor Pressure in lbs per ft^2.

INDEX OF PHOTOGRAPHS

Fig.	Condition of Test.	σ_n	H. m/mR3	Q. Degrees	T. Lbs.	Screen
1.	Cavitating.	0.6	49	23.9	120.8	Free Water
2.	"	0.7	352	9.0	18.7	" "
3.	"	0.7	50	25.3	128.0	" "
4.	"	0.8	56	26.5	134.3	" "
5.	"	0.9	53	28.3	144.8	" "
6.	Non-cavitating.	-	103	35.6	206.4	II.
7.	Cavitating.	0.5	121	17.8	87.3	II.
8.	"	0.7	108	23.0	201.5	II.
9.	"	0.9	52	28.5	157.2	II.
10.	"	0.7	115	21.4	103.7	VI.
11.	"	1.0	271	22.3	102.8	VI.
12.	"	1.3	338	22.5	108.5	VI.
13.	Non-cavitating.	-	70	39.2	132.5	VII.
14.	" "	-	154	32.4	183.1	VIII.
15.	" "	-	96	37.0	216.9	VIII.
16.	Cavitating.	0.7	152	20.4	94.9	"
17.	"	1.3	223	26.8	134.4	"
18.	"	1.6	370	18.6	90.8	"
19.	Apparatus:	Screens in nozzle and Pitot Tube.				
20.	" :	Torque and Tachometer.				
21.	" :	Thrust gage arrangement.				
22.	" :	Switchboard and Velocity Gages.				
23.	" :	Velocity Gages.				
24.	" :	Velocity Gage Ranges.				
25.	" :	Valves and Tunnel.				
26.	" :	Valve - Details on Tunnel.				

A C K N O W L E D G M E N T S.

I wish to thank the following persons for the great help they gave me in the preparation of this thesis:

Professor F.M. Lewis, for the suggestion of the topic of this thesis and for his advice and construct-:ive criticism.

Ray Johnson, for helping me run the tests in the Propeller-Tunnel and building a special attach-:ment on the nozzle of the tunnel which made it possible for me to run a greater number of tests with less time loss in exchanging screen arrangements.

Professor Walsh, for the use of his dark room and equipment which made it possible for me to process the large number of pictures and photostats myself.

H. MACH.

SYMBOLS USED

J.	Dimensionless Velocity Coefficient.
V.	Velocity.
N.	R.P.S. = Revolutions per second.
R.	R.P.M. = Revolutions per minute.
D.	Diameter of Propeller.
H.	Head of Bromobenzine or Hg-Velocity Gage.
μ.	Temperature Correction Factor for Bromo-:benzine Velocity Gage.
R.I,II & III.	Range Constants for Velocity Gage.
T_{cor}	Propeller Thrust, corrected for Hub Diameter.
ς	Density of Water.
K_t	Dimensionless Thrust Coefficient.
K_q	Dimensionless Torque Coefficient.
Q_{cor}	Propeller Torque angle corrected for Gage errors.
e	Propeller Efficiency.
σ_n	Cavitation Constant.
P_t	Absolute Tunnel Pressure.
P_v	Vapor Pressure.
T_g	Bromobenzine gage - Temperature.
T_t	Water Temperature in Tunnel.
η_{rr}	Relative Rotative Efficiency.

STATEMENT OF PROBLEM AND PURPOSE

The conditions under which model ship Propellers are usually tested in the Propeller Tunnel do not take into account the fact that the velocity distribution over the disc of the propeller on the full-size ship is irregular, due to the wake stream of the hull and propeller shaft fittings.

The purpose of this thesis is to determine the influence of a known variation of wake on the relative rotative efficiency of the propeller, both under non-cavitating and cavitating conditions.

EQUIPMENT USED.

Propeller Tunnel: For measurement of water velocity, Torque, Thrust, R.P.M. of propeller.

Propeller: #55: A 4-blade propeller of standard ogival blade section was used throughout the tests:

P/d =	1.005	m.w.R. =	.25
d. =	.989 ft.	B.T.F. =	.05
p. =	11.92"	R.P.M. =	1200.

Pitot-Tube: For determining the velocity distribution over the propeller disc as caused by wire mesh screens mounted in front of propeller.

Wire Mesh Screens and Support Cross: The wire mesh screens were attached to a brass cross by the means of thin wire. The support cross had to be changed two times during the tests and consisted of two brass bars 1/16" thick and 2" wide for the first support; 2 similar bars 1/8" thick and 2" wide for the second support. The two bars were soldered together at their centers to form a cross. The sections of the bars were shaped into an air foil section in order to minimize the influence on the water velocity.

The reason for changing the thickness of the bars from 1/16" to 1/8" was that the first arrangement proved to be insufficiently strong to hold against the considerable pressure caused by the high resistance of the wire mesh screens. The first arrangement was used for screen tests I,II,V.; the second arrangement for screen tests VI, VII.

For the last screen tests, VIII, the cross was reinforced by soldering a "T" shaped support into one quadrant as shown on Plate 7. The "T" was made from brass bars 1/16" thick and 2" wide.

Strobo - Flash Unit and Camera: For obtaining pictures of cavitation on propeller blades while running tests. The short duration of the flash

produced by the Strobo-Flash Unit, approximately 1/10,000 sec., practically stops the motion and makes it possible to investigate the differences of appearance of cavities on different blades, caused by irregular wake distribution.

- P R O C E D U R E -

Part A: Non-Cavitating Tests.

I. The first test was run without any screens (free water tests) in the discharge nozzle of the propeller tunnel, under non-cavitating conditions. Its purpose was to determine reference curves of the dimensionless torque and thrust coefficients K_q and K_t versus the dimensionless velocity co-:efficient J.

The procedure during the actual tests was to keep the propeller R.P.M. constant at 1200 R.P.M., and varying the water velocity in the tunnel in such a manner as to obtain data in a range from "no load condition" (T = 0 lbs) to "full load condition".

Measurements of H,Q and T were taken in small intervals of 5 to 10 lbs thrust. With these data the dimensionless coefficients K_t, K_q and J and the propeller efficiency were calculated and plotted.

II. The second series of tests were run with screen arrangement I., consisting of 3 concentric circular screens of diameters 7", $4\frac{1}{2}$" 3" respectively,, mounted on the discharge nozzle of the tunnel (see Fig.19)

First, it was necessary to obtain the velocity distribution over the propeller disc which

was accomplished with a pitot tube mounted temporarily on the tunnel. During these tests, the propeller and hub had to be removed from the propeller shaft in order to get velocity readings close to the center of the disc. The purpose of these pitot tube tests was not as much to obtain the exact water velocities at each point of the propeller disc, but rather to obtain a distribution curve for two water speeds taken at random (corresponding to a head of H = 200 m/m and H = 400 m/m). From the resulting plots it was seen that the water speed had a practically negligible effect on the distribution of velocity for one certain screen arrangement.

The second run was made with the propeller and hub in place, non-cavitating at 1200 R.P.M. in the same manner as the first test (I). In plotting the "K_t" and "K_q" curves, however, a new method had to be adopted because the velocity indicated by the head on the manometer (Bromobenzine gage), "H", was not any more the actual velocity at every point of the propeller, but rather an overall velocity in the nozzle before the water reached the screen obstructions. In order to make a comparison of the coefficients "K_t" and "K_d" with those of the "free water run" possible, which was necessary to obtain the relative rotative efficiency, the following method of plotting these curves was used:

The calculated "K_t" value of the screen test was entered in the free water test curve "K_t" and the corresponding J value read from the free water plot. The "K_q" of the screen test was then plotted against this J on the same sheet used for the free water plot (Plate 12). The resulting curve of "K_q" versus J did not coincide with the free water "K_q", but all"K_q" values were somewhat lower than in the free water run. In the following a certain number of J values were chosen and the corresponding "K_q" values read from the curves. The relative rotative efficiency was then obtained by forming the ratio of the screen test "K_q" over the free water test "K_q"

$$\text{i.e. } \eta_{R.R.} = \frac{K_q \text{ with screens}}{K_q \text{ free water.}}$$

and plotted versus J. (Plate 12).

III. In the following non-cavitating tests the same procedure for obtaining the relative rotative efficiency was applied for the rest of the screen arrangements in the following order:

1) Screen arrangement II, consisting of two con-:centric circular screens of 10" and 7" diameter respectively.
2) Screen arrangements III and IV which were abandoned.
3) Screen arrangement V, consisting of one

circular screen of 12" diameter and one concentric circular ring screen with 12" outside diameter and 8" inside diameter.

4) Screen arrangement VI, consisting of one half circle screen of 5" radius and one concentric half circle ring with 3" inside radius and 5" outside radius.

5) Screen arrangement VII, consisting of one half circle screen of 5" radius and one concentric half circle screen of $3\frac{1}{2}$" radius.

6) Screen arrangement VIII, consisting of 3 screens of 2", 3", 5" width, arranged in one quadrant of the support cross as indicated on Plate 7.

In running the test with screen arrangement V, great difficulty was encountered in the form of too high water pressures on the support cross with full R.P.M. (1200). This test had, therefore, to be conducted with half R.P.M. (600) and half speed of tunnel because the support collapsed whenever a velocity of over about 12 feet per second of the water in the tunnel was reached. This also caused me to build a stronger support cross with $\frac{1}{8}$" brass bars instead

of 1/16". This second cross stood up very well under the pressure and did not show any visible deformation as did the first one.

Part B: Cavitating Tests.

L. As in the non-cavitating tests, the first series of cavitating runs were made with no screens mounted in the tunnel nozzle (free water). These tests were made for the same reason, i.e., to obtain curves of "K_t", "K_q" versus J., as a basis for comparison and to obtain the relative rotative efficiency under different conditions of wake distribution. Runs were made with the following cavitation constant σ_n :

σ_n =	0.5	$P - P_v$ =	68.0	m/m Hg.
" =	0.6	$P - P_v$ =	81.6	m/m Hg.
" =	0.7	$P - P_v$ =	95.2	m/m Hg.
" =	0.8	$P - P_v$ =	108.9	m/m Hg.
" =	0.9	$P - P_v$ =	122.3	m/m Hg.
" =	1.0	$P - P_v$ =	135.4	m/m Hg.
" =	1.3	$P - P_v$ =	176.1	m/m Hg.
" =	1.6	$P - P_v$ =	216.8	m/m Hg.

For each of these runs, curves of K_t and K_q versus J were plotted together with the non-cavitating run K_t and K_q curves, which served as reference and check, as the cavitating curve with the highest σ_n (= 1.6) had to touch this curve or come very near to it. The reason for this is that at high σ_n values and high ($P - P_v$) which condition corresponds with a low vacuum (close to non-cavitating condition), the propeller operates non-cavitating for a short range of medium water speed.

In addition to the K_t and K_q versus J curves

the velocity gage readings, "H", were plotted versus the calculated "J" which later served as a basis for plotting the K_t and K_q curves of the screen tests.

II. The second series of cavitating tests were run with the following screen arrangements:

1) Screen arrangement I for σ_n = 0.8; but as it did not show any noticible effect in the non-cavitating runs, this screen arrangement was abandoned.

2) Screen arrangement II for σ_n = 0.9, 0.8, 0.7, 0.6, 0.5. These data, however, were not used, as the main interest in the cavitating tests lay in the next screen arrangements, VI and VIII.

3) Screen arrangement VI and VIII for the following cavitating constants:

σ_n =	0.5	$P - P_v$ =	67.6 m/m Hg.
" =	0.7	$P - P_v$ =	94.5 m/m Hg.
" =	1.0	$P - P_v$ =	135.1 m/m Hg.
" =	1.3	$P - P_v$ =	175.7 m/m Hg.
" =	1.6	$P - P_v$ =	216.1 m/m Hg.

Here again, like the non-cavitating screen test, a special method of plotting K_t and K_q coefficients had to be used in order to get curves under the same velocity conditions as in the free water cavitating runs. This method of plotting the K_t and K_q coefficients is described in the followimg:

a) The "H" reading of the non-cavitating screen tests were plotted against the calculated J values.

b) The calculated K_t values of the non-cavitating screen tests were plotted against the J values.

c) The calculated K_t values of the cavitating screen tests were plotted against J determined from the plot of H versus J using the J values corresponding to the H value read from the gage.

d) The calculated K_q values of the cavitating screen tests were plotted against this same J value used for the K_t curves.

Part C: Pictures.

Through all the tests but with special emphasis on the cavitating tests, I took photographs of the propeller in order to obtain lasting records of the sometimes very interesting changes in appear-:ance and form of cavities on the blades of the propeller.

DISCUSSION OF RESULTS

Part A: Non-cavitating Tests.

The results of the non-cavitating tests are plotted on Plate 12.

I) The highest relative rotative efficiency was reached with screen arrangement V. With this increasing wake towards the tips of the propeller blades (See Plate 3) the relative rotative efficiency lies about $\frac{1}{2}$% above 100%. At low water speed represented by low J values, however, the relative rotative efficiency drops off and reaches 95% at J = 0.4. This indicates that at low water speed and high load the screen has less influence on the relative rotative efficiency, which is also evident from all other screen arrangements. All screen arrangements approach 100% relative rotative efficiency at low J values.

II) The next highest relative rotative efficiency was attained with Screen I in front of the discharge nozzle. This was to be expected because of the rather small diameter of the screens used. They do not have much influence on the wake distribution towards the propeller tips; most of the wake is concentrated at the hub (See Plate I). From this it can easily be deduced that the wake caused by propeller shaft and shaft fittings on a full size ship has very little influence

on the relative rotative efficiency of the propeller.

III. The next screen arrangement showing a slightly lower relative rotative efficiency than screen I is screen VIII. This case of an increasing wake towards towards the tips of the propeller blades (See Plate 6), represents more or less closely the actual wake dis-:tribution on a twin-screw ship. The screens in this case cover only one quadrant of the propeller disc. The lowest relative rotative efficiency with screen VIII was reached with high J values, being 93% at J = 1.0. With still higher J values, the curve rises very sharply towards 100% and even above, which seems to indicate, that at high water-speed the wake distribution changes somewhat from the one indicated on Plate 6, in such a manner, that this wake distribution approaches more the case of screen V.(Another explanation of this rather odd rise in relative rotative efficiency is the un-:certainty of the test results at low torque and thrust, especially with this screen arrangement, which caused the torque and thrust to fluctuate over a wide range.)

IV. The screen arrangement II, with an increasing wake towards the propeller hub (See Plate 2), results in an almost constant relative rotative efficiency over the whole range of J values. The relative rotative efficiency varies from 89.5% at J = 0.4

to 91% at J = 0.96. For higher J values the relative rotative efficiency drops off and reaches 84.5% at J=1.1. Again, this sudden change might be caused by fluctuating torque and thrust reading, at high water speed.

V). Screen VI, which covered half of the nozzle exit and had an increasing wake towards the tips of the propeller blades (See Plate 4), resulted in a still lower relative rotative efficiency than screen II at high J values. H reaches its minimum value at J = 1.1 with relative rotative efficiency of 82.5%. At low J values, the curve approaches 100% relative rotative efficiency much more than any other screen arrangement which can be explained as under item I.

VI) Screen VII, which covered half of the dis-:charge nozzle had, however, an increasing wake towards the propeller hub (See Plate 5). This results in the lowest relative rotative efficiency of all screen arrangement, reaching 81% at J = 1.1. At low J, like all other screen arrangements, the curve approaches 100% relative rotative efficiency, but slower. Its maximum value of 99% is attained at J = 0.4.

Part B: Cavitating Tests.

The results of the cavitating tests are represented in Plates 13 to 18.

Comparison between Plates 13, 15, 17, which show K_t values versus J of free water test, screen VI and screen VIII, respectively shows that for all cavitation constants σ_n the curves for screen VI lie below the ones for free water. For screen VIII the curves are very close to those of screen VI, but still somewhat lower. This is due to the effect of the screens on the formation of cavities on the propeller blades, which is more closely discussed under Part C, discussion of pictures.

Comparison between Plates 14,16 and 18, representing K_q versus J, show the same effect of the screens on the cavities formed on the blades. However, in this case, the differences are smaller than those of the K_t versus J values.

The reason thereof is, that the formation of cavities on the propeller blades has more influence on the thrust than on the torque of the propeller (as indicated by dimensionless coefficients K_t and K_q respectively.)

Part C: Discussion of Pictures.

Fig. 1., shows the appearance of cavitation at σ_n = 0.6 under free water conditions (no screens in discharge nozzle). The picture was taken at full load corresponding to minimum water speed and maximum torque.

Fig. 2., shows cavitation at σ_n = 0.7 free water. The picture was taken at high water speed (H = 352 mm R3). Note that cavities are distributed evenly over all blades.

Fig. 3., shows cavitation at σ_n = 0.7 but full load free water. The picture was taken to show that the appearance of cavities does not change with changing cavitation index σ_n . Comparison with Fig. 1., shows no visible difference at all.

Fig. 4., shows cavitation at σ_n = 0.8, free water. Again comparison with Fig. 1., shows no difference, except that cavitation is less heavy on Fig.4., because of lower cavitation index .

Fig. 5., shows cavitation at σ_n = 0.9, free water. Again no visible difference.

Fig. 6., was taken under non-cavitating conditions with screen II, in the discharge nozzle. The picture shows very clearly the tip-vortices and the contraction of the propeller race.

Fig. 7., shows cavitation at σ_n = 0.5, with

screen II. There seems to be quite some change in comparison with the free water cavitation, but this is due to the lower cavitation index.

Fig. 8., shows cavitation at σ_n = 0.7 with screen II. Here the change in appearance of the cavities is very visible. The picture was taken at high load, still, there is only a small amount of cavitation on the blade-tips. The explanation seems to be that screen II defers cavitation.

Fig. 9., showing cavitation at σ_n = 0.9 with screen II is similar to Fig.5., but cavitation near the propeller tips is heavy.

Fig.10., shows cavitation at σ_n = 0.7 with screen VI. Here we can see the difference in cavitation between blades "u" and "m". The strong wake in the upper half of the disc causes the upper blades "m" to cavitate much heavier than the lower blades "u".

Fig.11., shows cavitation at σ_n = 1.00 with screen VI. Because of higher cavitation index the cavitation is not as heavy as in Fig.10. While blade "m" is cavitating heavily in the upper part (where strong wake starts) cavitation decreases towards the leading edge, which lies still in a region of low wake velocity. Blade "u" cavitates much less than "m" lying in a region of maximum water velocity.

Fig. 12., shows cavitation at σ_n = 1.3 with screen VI. Again like in Fig.10 and 11, the upper blade "m" cavitates on the face, while "u" does not show any face cavitation. Right behind the trailing edge of "u" some cavitation appears, which results from the back cavitation on this blade (not visible on this picture).

Fig. 13., shows the formation of tip vortices and propeller race under non-cavitating conditions. Note how race becomes irregular on top of picture, caused by stronger and irregular wake of screen VII.

Fig. 14., shows the difference of tip vortices even clearer than Fig.13; non-cavitating screen test VII.

Fig. 15., was taken under non-cavitating conditions with screen VIII. The heavy tip vortices show the position of the screen very clearly.

Fig. 16., shows cavitation at σ_n = 0.700 with screen VIII. This picture shows very clearly the great influence of a strong wake near the propeller tips. The screen lies in front of blade "u". Note how cavities of blade "b" at bottom of picture disappear in region II, but appear again in region I under the influence of a strong wake.

Fig. 17., shows the same effect as Fig. 16.,

but is taken at σ_n = 1.3 with screen VIII.

Fig.18., shows cavitation at σ_n = 1.6 with screen VIII. Here the influence of strong wake is very clearly visible on blade "m". This blade is cav-:itating quite heavily, while blade "u" shows just the beginning of some cavitation at the tip in region I., however, the propeller race cavitates again. Note also the abrupt beginning of cavitation on blade "m". This case is probably closest to the actual condition on a twin screw ship, where the propeller tips work in a wake caused by the hull.

Fig.19 - 26., show parts of the apparatus in the propeller tunnel.

RECOMMENDATIONS.

As recommendation for future investigation on the influence of wake variation over the propeller disc, I could suggest, that tests be run with screens similar to those used in this thesis, but giving the water at the nozzle exit a circular motion by means of guide blades.

It might also prove very interesting to find a theoretical solution to this problem, which would make it possible to predict more or less accurately, the relative rotative efficiency for different wake variations.

SAMPLE CALCULATIONS.

Data A:

H = 541 mm (Bromobenzine Gage) R3.

Q = 10.8 Degrees. T_t = 61° F.

T = 4.4 Lbs. RPM = 1200.

T_g = 77° F. d = .9855.

I) Tunnel Constants:

a) Correction factor for Bromobenzine gage:

at T_g = 77°F: = 0.999 (From Plate..8....)

b) Thrust correction:

At T = 4.4 lbs: corr = 0.7 (From Plate..9....)

c) Density of Water:

At T_t = 61°F: = 1.9381 (From Plate..10....)

d) Torque Correction: = -4.0°

2) Velocity of Water in Tunnel V:

V = (Range Constant) $x\sqrt{\rho \cdot H}$ =

= 0.94052 $\sqrt{0.999 \cdot 541}$ = 21.96 ft/sec.

3) Velocity Coefficient J:

$$J = \frac{V}{n \times d} = \frac{60\ V}{R.d} = \frac{60 \cdot 21.96}{1200 \cdot 0.9855} = 1.105$$

4) Thrust Coefficient K_t:

$$K_t = \frac{T_{corr}}{\rho \cdot n^2 \cdot d^4} = \frac{4.4 \quad 0.7}{1.9381 \times 20^2 \times 0.9855^4} =$$

$$= \frac{5.1}{1.9381 \times 400 \times 0.942} \quad \therefore \quad \underline{K_t = 0.00695}$$

5) Torque Coefficient K_q:

$$\underline{K_q} = \frac{Q_{corr}}{\rho \times n^2 \times d^5} = \frac{=10.8 - 4.0}{1.9381 \times 20^2 \times 0.9855^5} =$$

$$= \frac{6.8}{1.9381 \times 400 \times 0.93} = \underline{0.00944}$$

6) Efficiency :

$$= \frac{J \times K_t}{2\pi \times K_q} = \frac{1.105 \times 0.00695}{2\pi \times 0.00944} = \underline{14.4\%}$$

CAVITATING CONSTANT:

(For Screen VI)

$\sigma_n =$ 0.5

$$(P - P_v)^{lbs/ft^2} = \sigma_n \times \rho/2 \times n^2 \times d^2$$

$$(P - P_v)\ m/m\ Hg = \frac{(P - P_v)^{lbs/ft^2}}{2.7743} = \frac{\sigma_n \times \rho \times n^2 \times d^2}{2 \times 2.7743}$$

$$= \frac{0.5 \times 1.9339 \times 20^2 \times 0.9855^2}{2 \times 2.7743}$$

$$= \underline{67.6\ m/m\ Hg.}$$

PLATE 1.

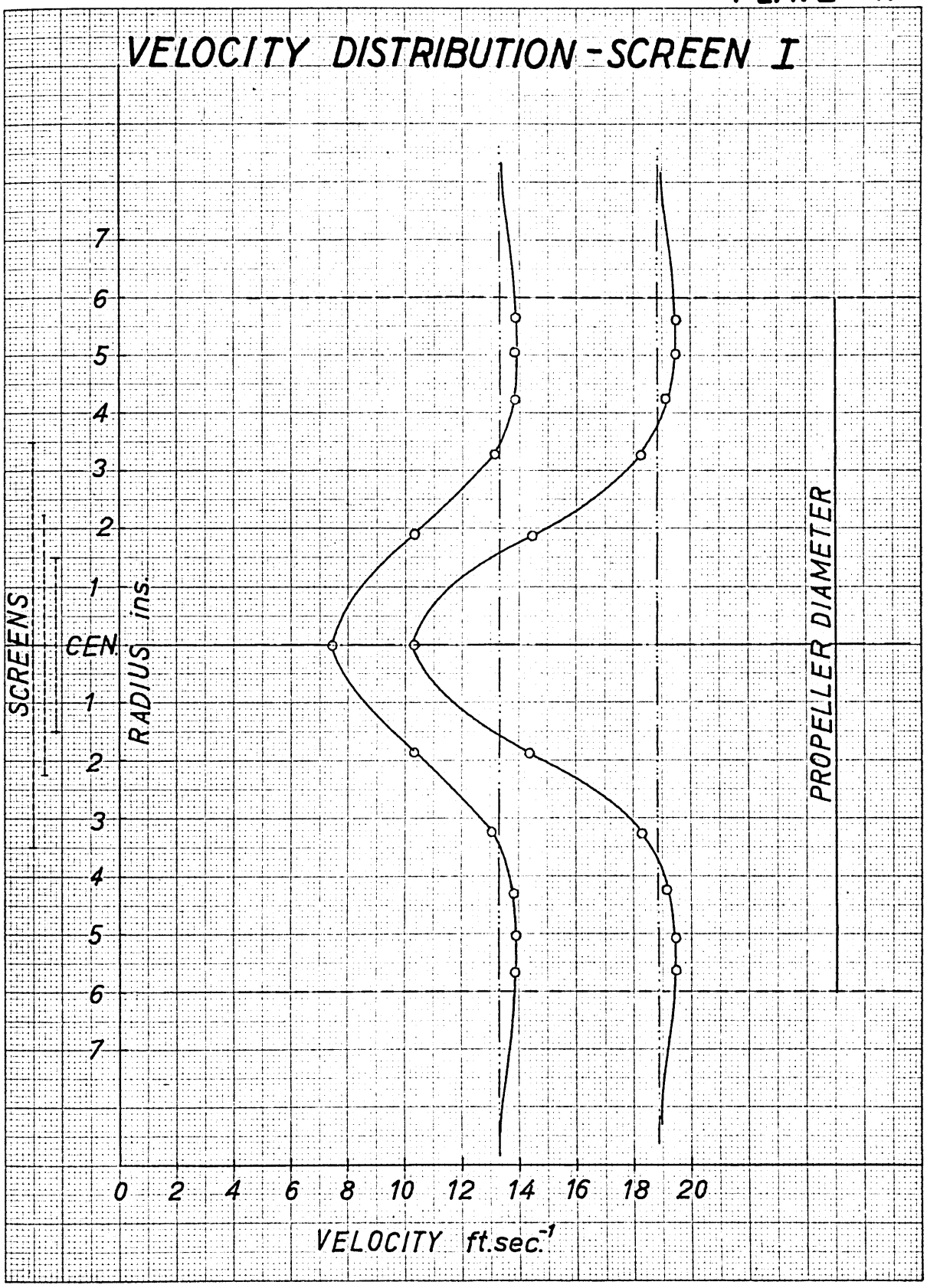
VELOCITY DISTRIBUTION - SCREEN I
7
6
5
4
3
2
1
CEN.
1
2
3
4
5
6
7
RADIUS ins.
SCREENS
PROPELLER DIAMETER
0
2
4
6
8
10
12
14
16
18
20
VELOCITY ft.sec.-1

PLATE 2.

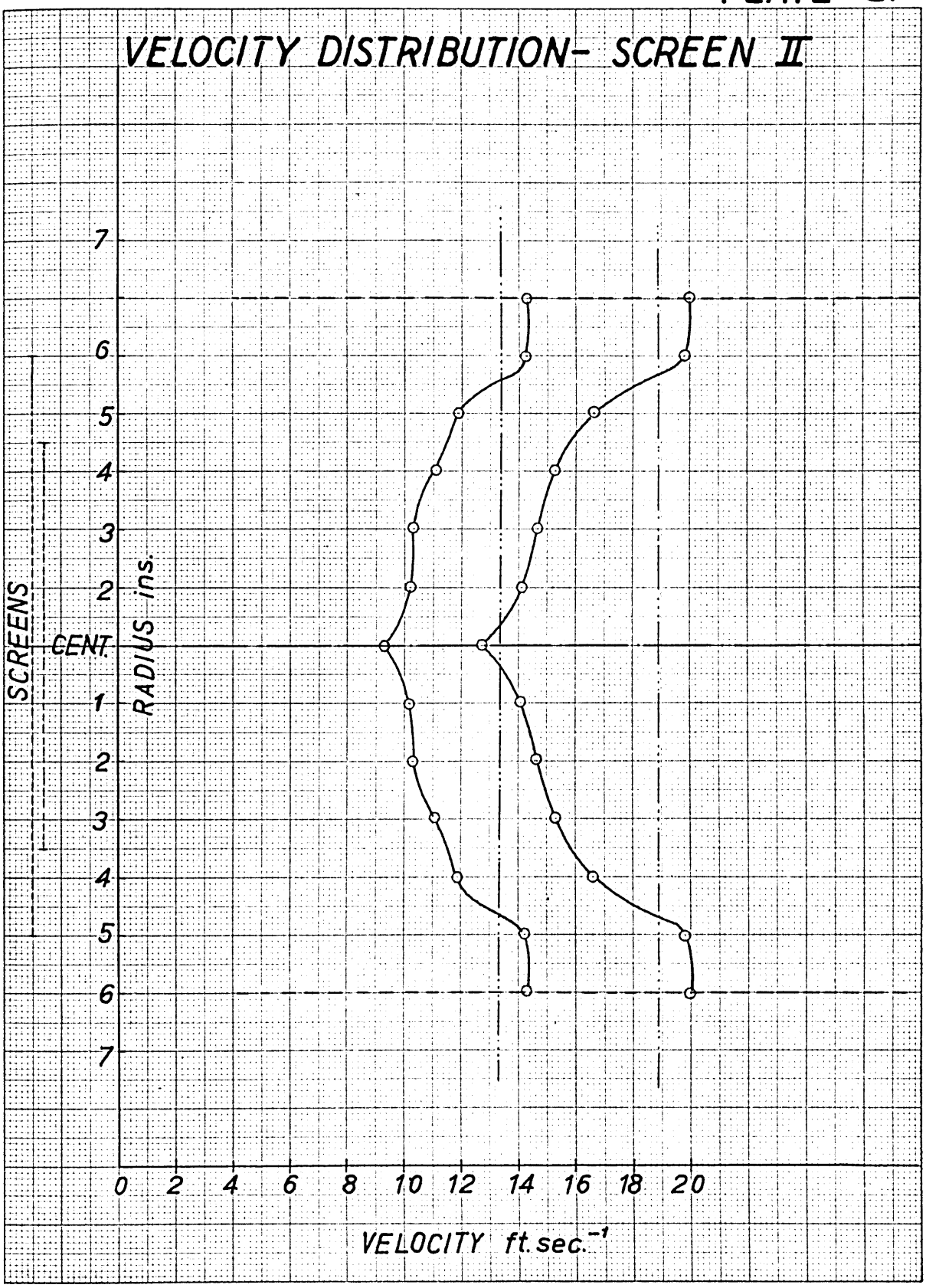
VELOCITY DISTRIBUTION- SCREEN II
SCREENS
CENT.
RADIUS ins.
7
6
5
4
3
2
1
2
3
4
5
6
7
0 2 4 6 8 10 12 14 16 18 20
VELOCITY ft. sec.⁻¹

PLATE 3.

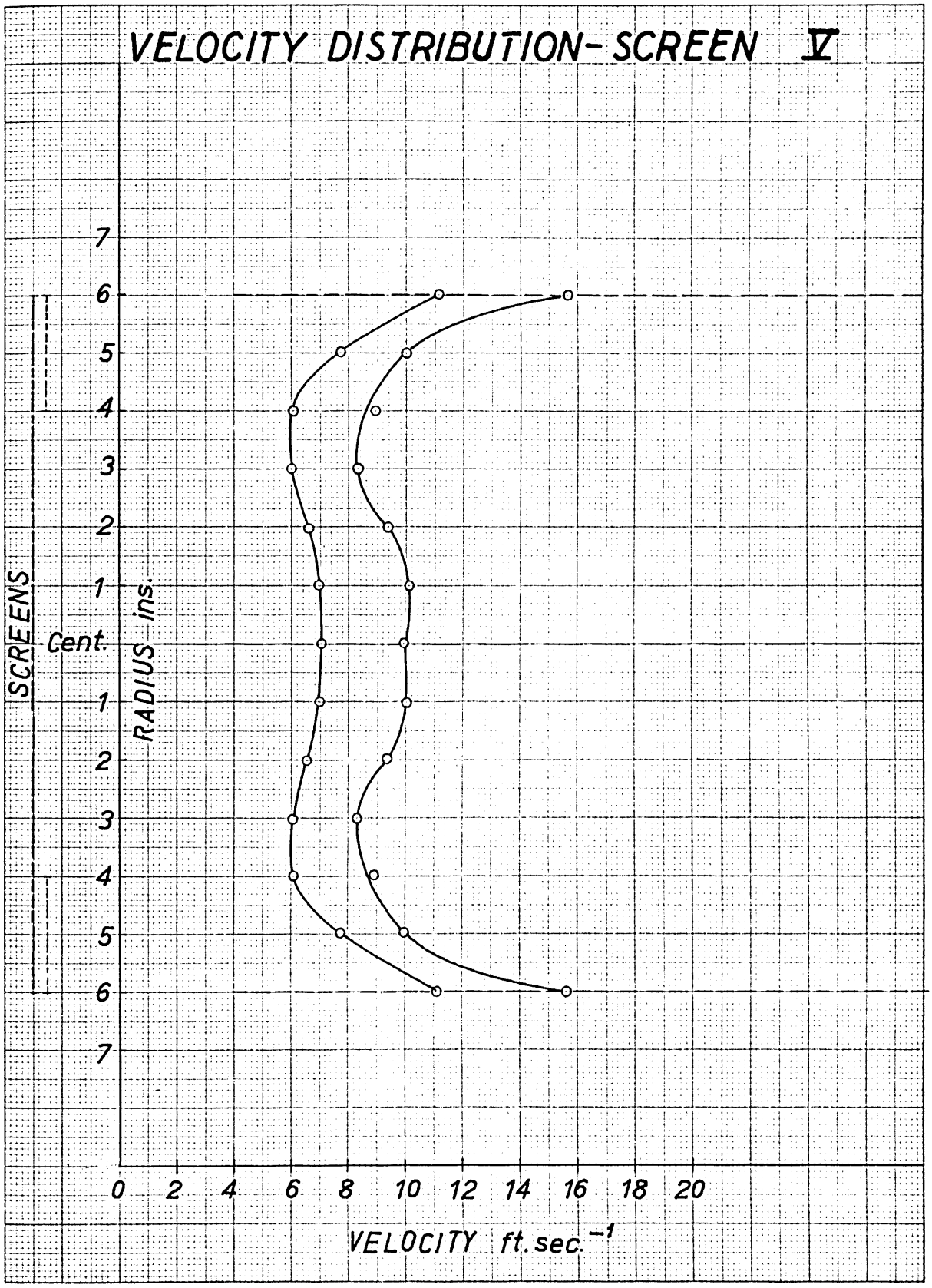
VELOCITY DISTRIBUTION- SCREEN V
SCREENS
Cent.
RADIUS ins.
7
6
5
4
3
2
1
1
2
3
4
5
6
7
0
2
4
6
8
10
12
14
16
18
20
VELOCITY ft. sec.⁻¹

PLATE 4.

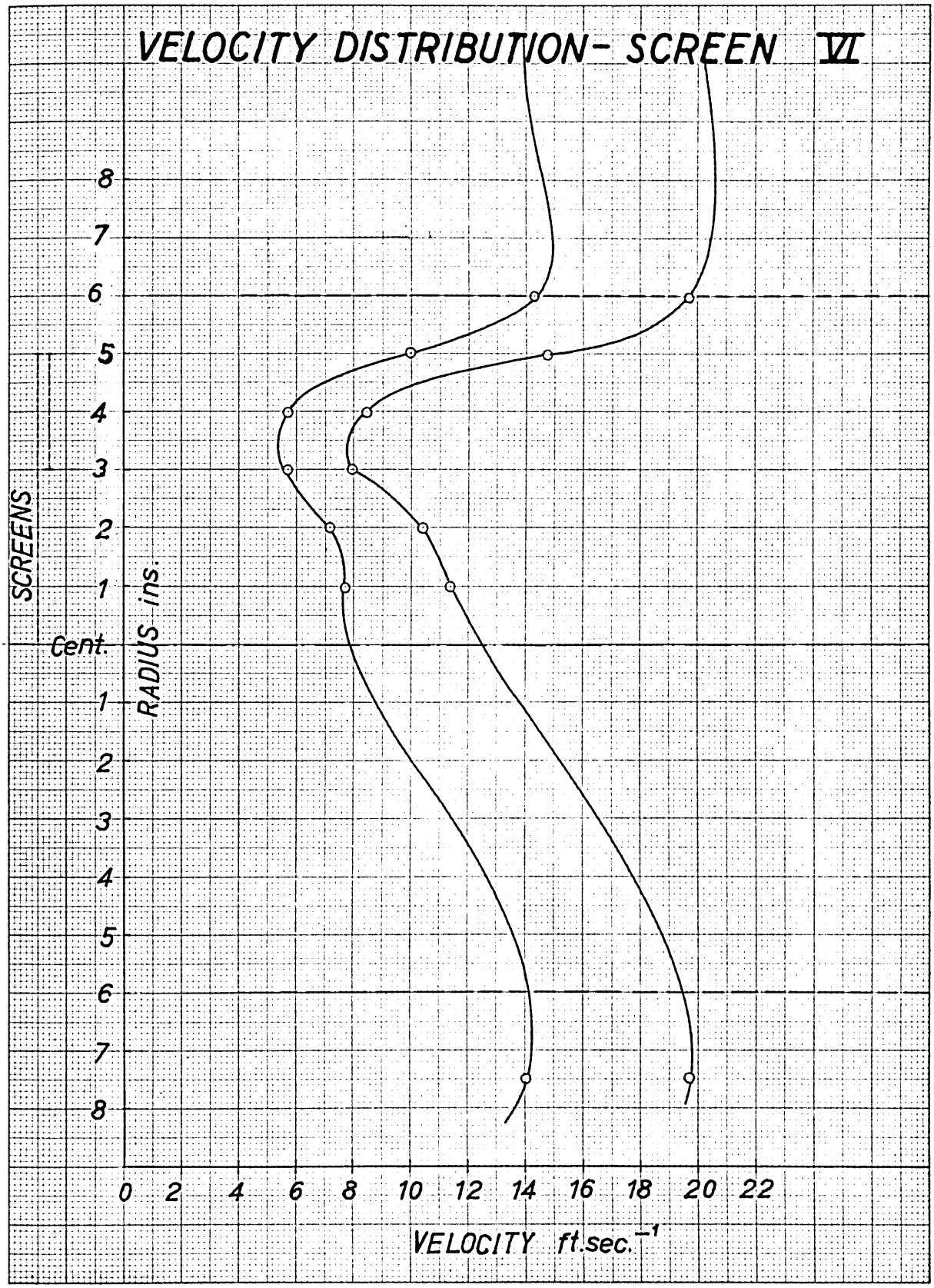
VELOCITY DISTRIBUTION- SCREEN VI
SCREENS
RADIUS ins.
Cent.
8
7
6
5
4
3
2
1
1
2
3
4
5
6
7
8
0 2 4 6 8 10 12 14 16 18 20 22
VELOCITY ft.sec.-1

PLATE 5.

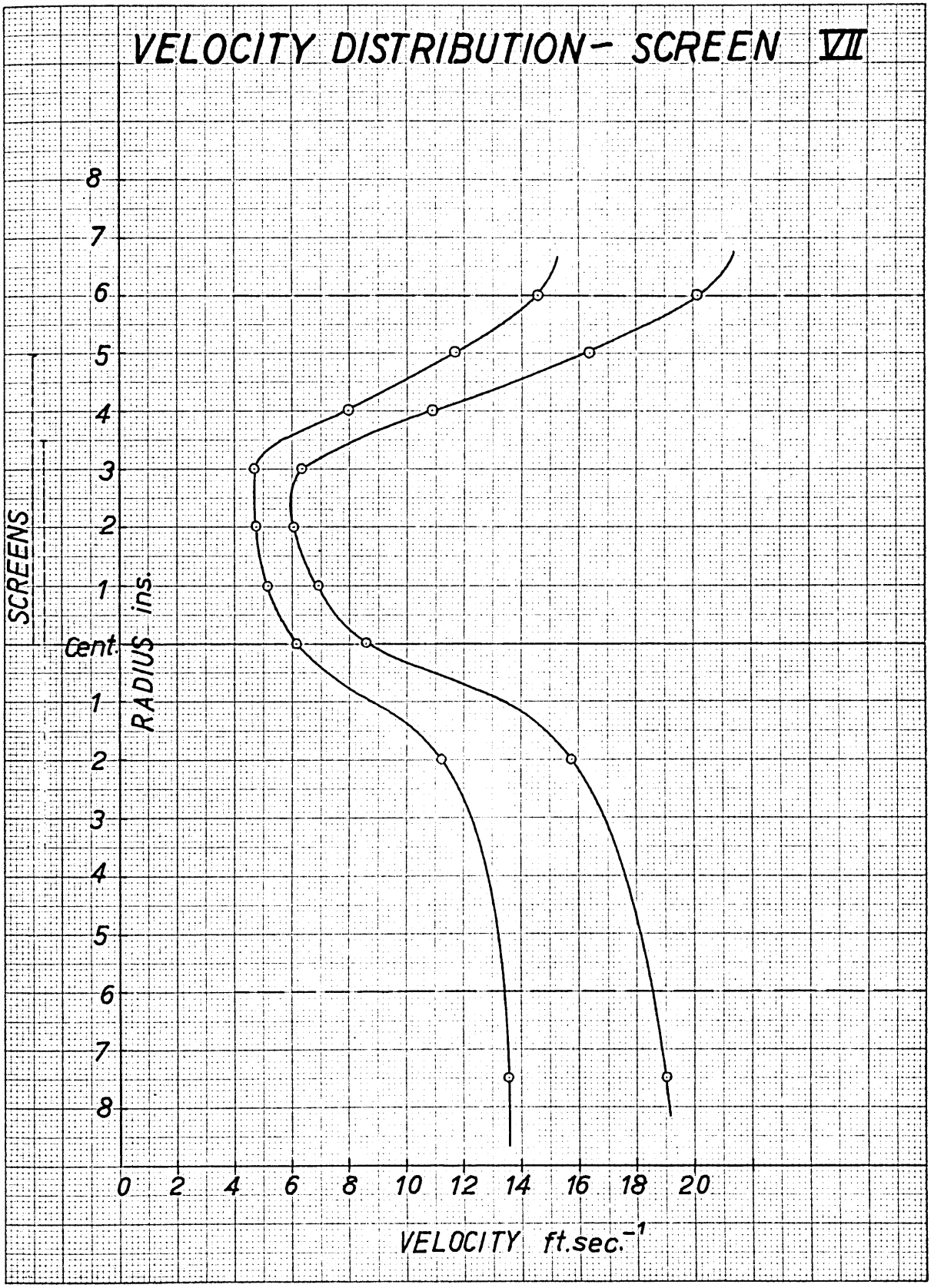
VELOCITY DISTRIBUTION- SCREEN VII
SCREENS
RADIUS ins.
Cent.
8
7
6
5
4
3
2
1
1
2
3
4
5
6
7
8
0 2 4 6 8 10 12 14 16 18 20
VELOCITY ft.sec.-1

PLATE 6.

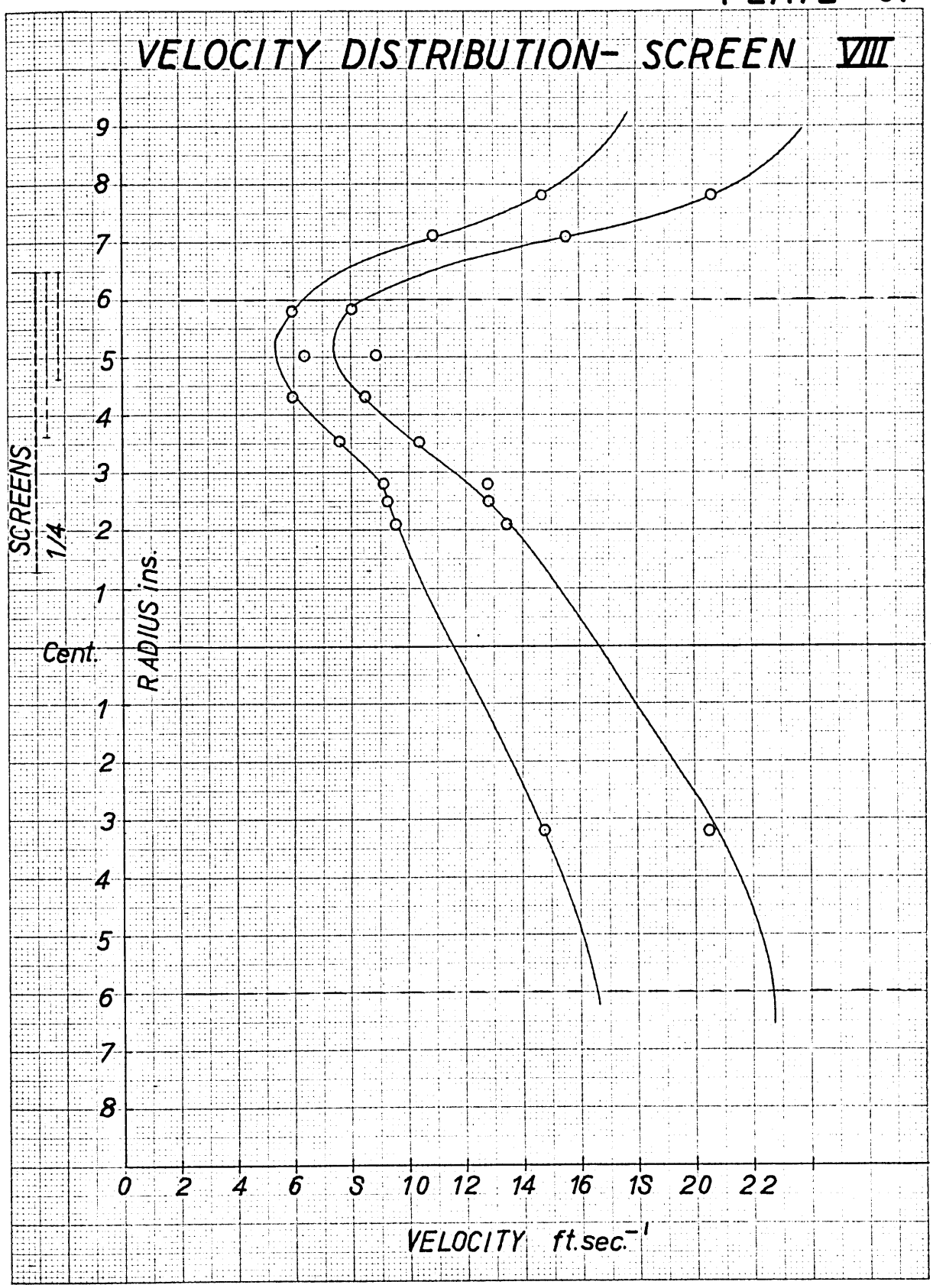
VELOCITY DISTRIBUTION- SCREEN VIII
SCREENS
1/4
Cent.
RADIUS ins.
9
8
7
6
5
4
3
2
1
1
2
3
4
5
6
7
8
0
2
4
6
8
10
12
14
16
18
20
22
VELOCITY ft.sec.⁻¹

PLATE 7.

SCREEN ARRANGEMENTS.

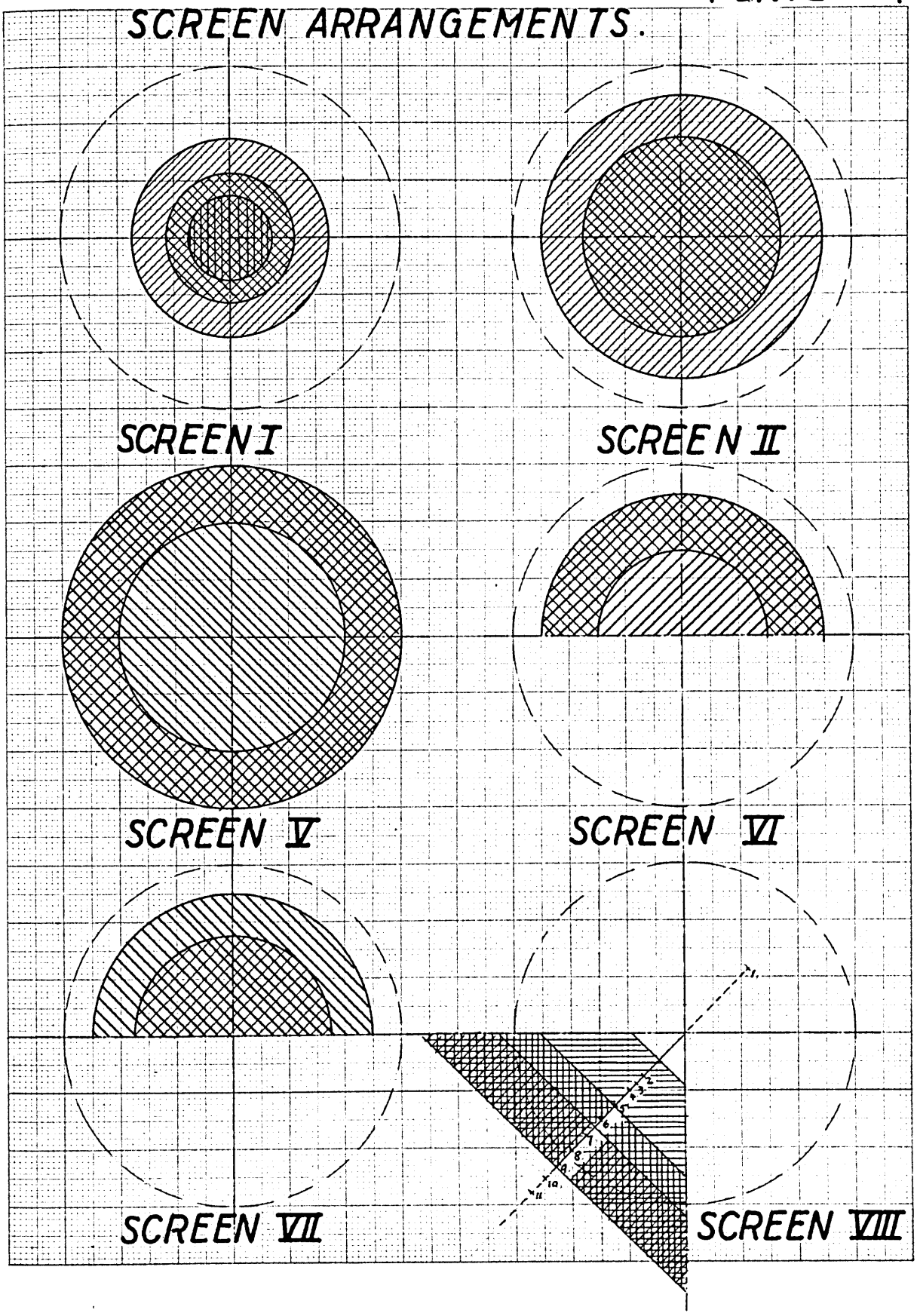

PLATE 8

TUNNEL CONSTANTS – VEL.GAGES –

Correction Factors of Bromo-Benz.Gage vs. Temperature.

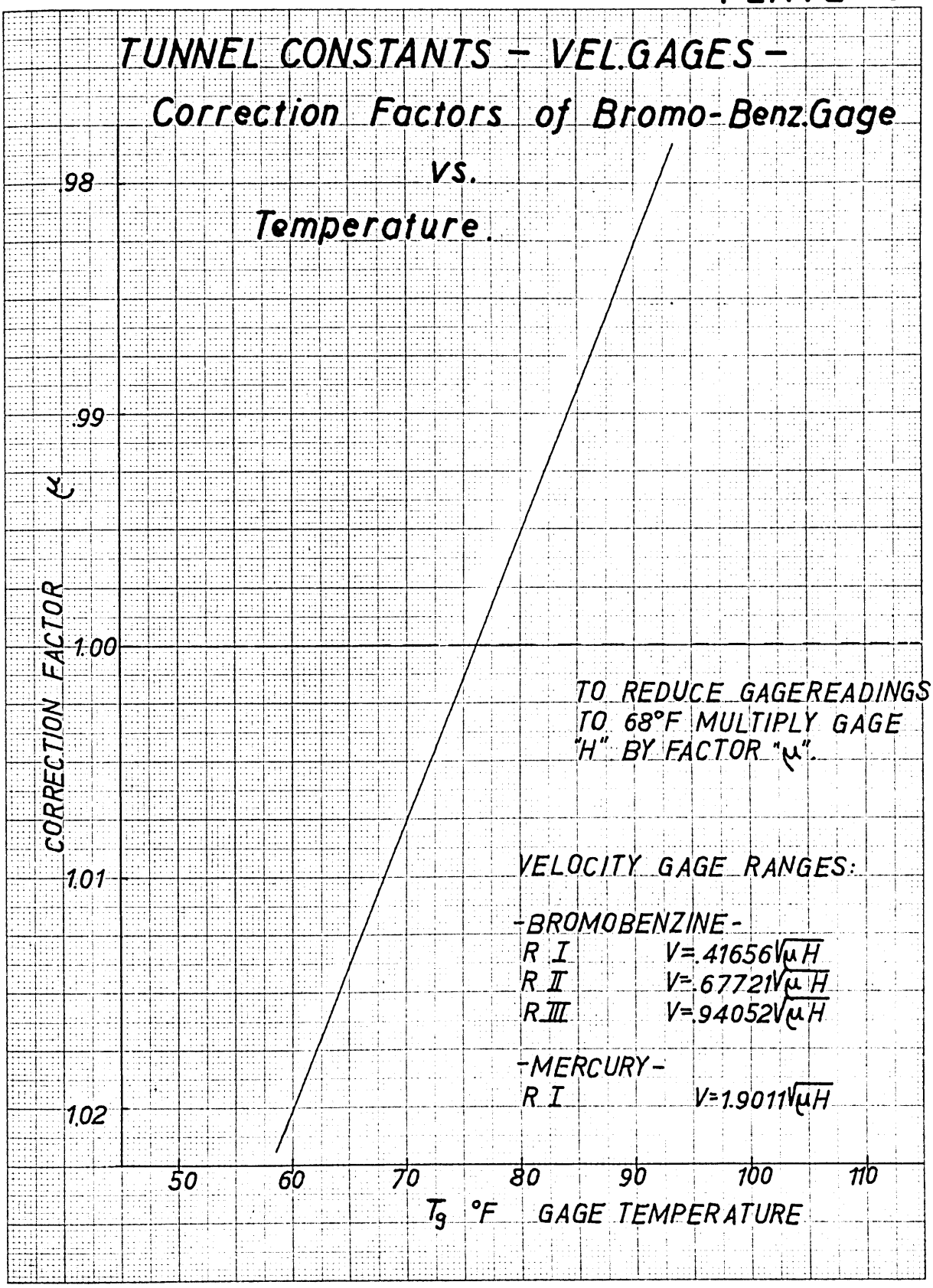

PLATE 9.

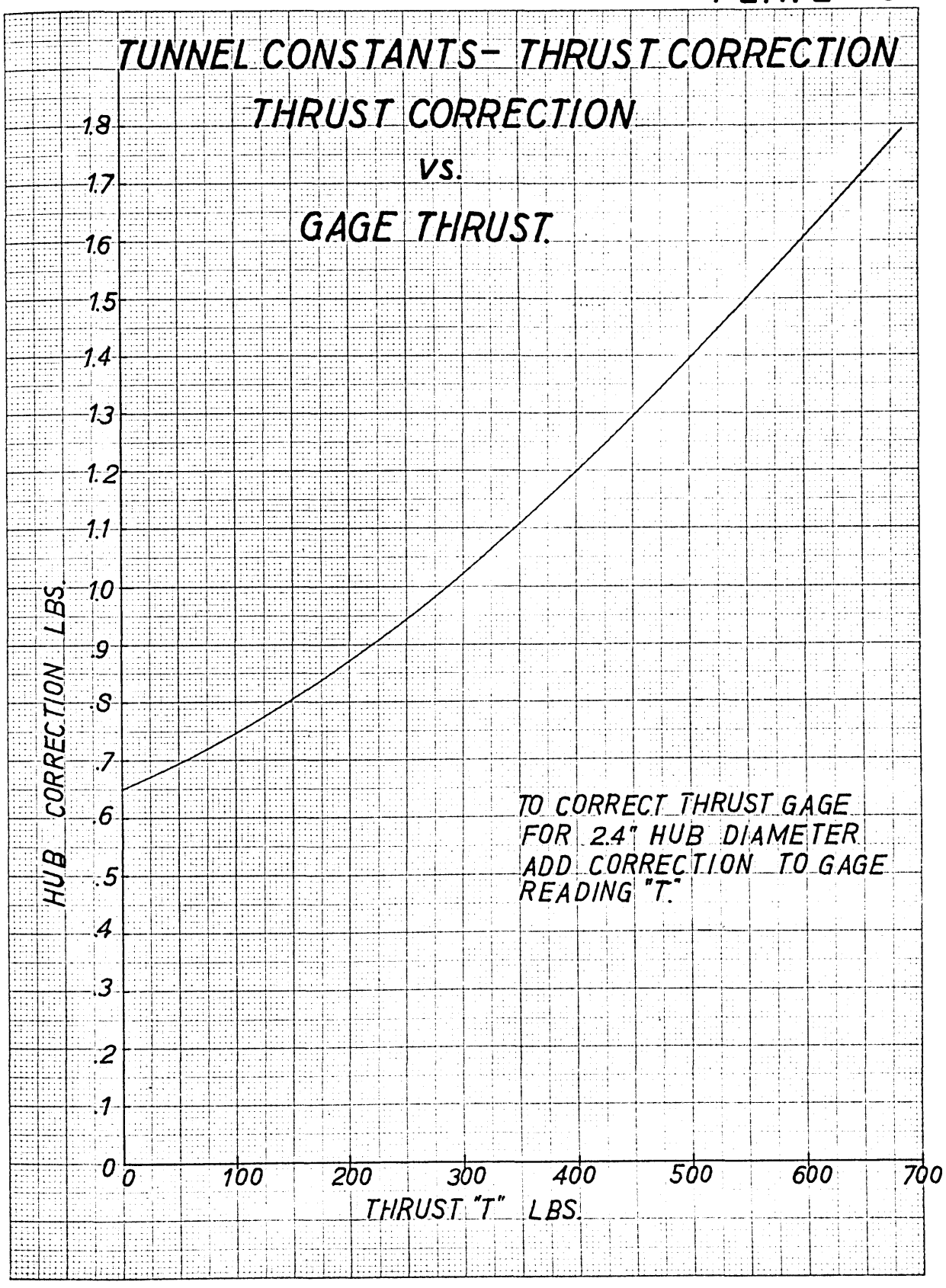
TUNNEL CONSTANTS- THRUST CORRECTION
THRUST CORRECTION
VS.
GAGE THRUST.
HUB CORRECTION LBS.
1.8
1.7
1.6
1.5
1.4
1.3
1.2
1.1
1.0
.9
.8
.7
.6
.5
.4
.3
.2
.1
0
0
100
200
300
400
500
600
700
THRUST "T" LBS.
TO CORRECT THRUST GAGE FOR 2.4" HUB DIAMETER ADD CORRECTION TO GAGE READING "T."

PLATE 10.

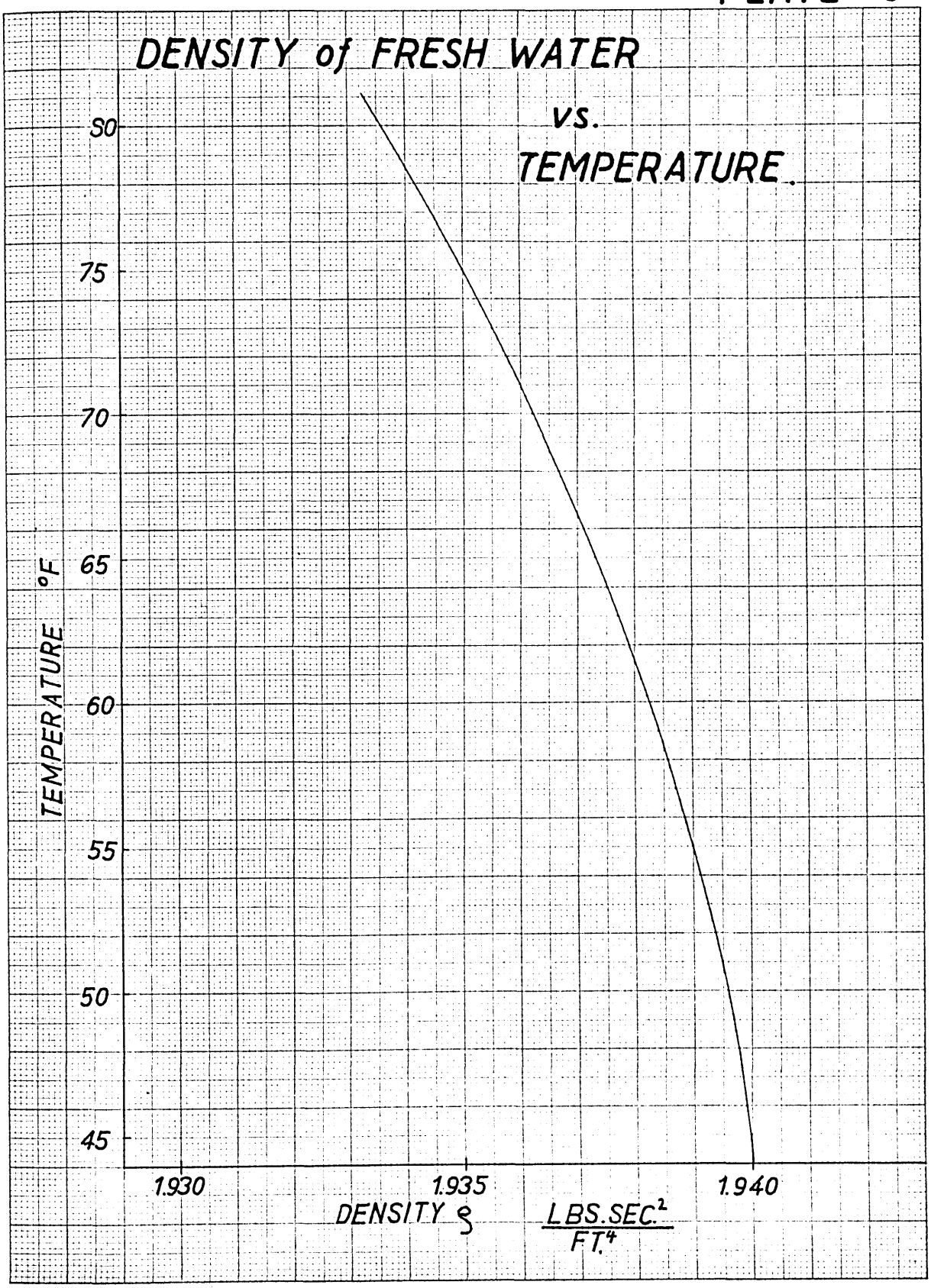
DENSITY of FRESH WATER
vs.
TEMPERATURE.
80
75
70
65
60
55
50
45
TEMPERATURE °F
1.930
1.935
1.940
DENSITY ρ
LBS. SEC.²/FT.⁴

PLATE 11.

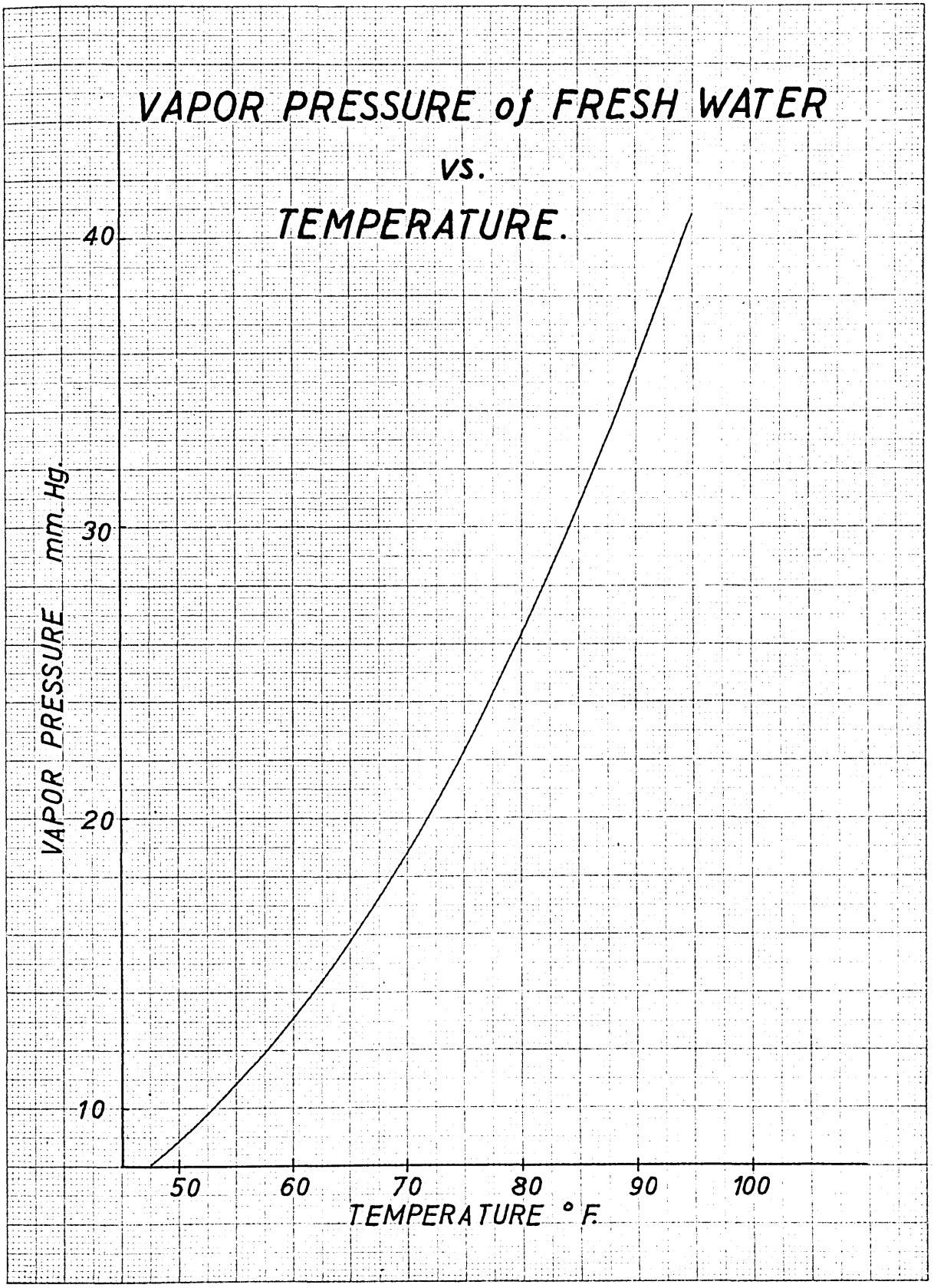
VAPOR PRESSURE of FRESH WATER
vs.
TEMPERATURE.
VAPOR PRESSURE mm. Hg
40
30
20
10
50
60
70
80
90
100
TEMPERATURE ° F.

PLATE 12.

Relative rotative Efficiency.

K_t x 10^{-1}.
K_q x 10^{-2}.

K_t and K_q

η_{rr}

K_q vs. J non cavitating.

K_t vs. J non cavitating.

V
I
VIII
II
VI
VII

OPEN WATER
SCREEN I
SCREEN II
SCREEN V
SCREEN VI
SCREEN VII
SCREEN VIII

SCREEN V
OPEN WATER
SCREEN VIII
SCREEN I
SCREEN II
SCREEN VI
SCREEN VII
OPEN WATER

J

KEUFFEL & ESSER Co NEW YORK.

PLATE 13.

K_t vs. J cavitating.
Free water Test.

K_t

.4 .35 .30 .25 .20 .15 .10 .05 0

σ_n= 1.6

σ_n= 1.3

σ_n= 1.0

σ_n = .7

σ_n= .5

H vs. J NON CAV. FREE WATER.

K_t vs. J NON CAV. FREE WATER.

800 700 600 500 400 300 200 100 0

H m/m

.3 .4 .5 .6 .7 .8 .9 1.0 1.1 1.2 1.3

J

PLATE 14.

K_q vs. J cavitating.
Free water Test.

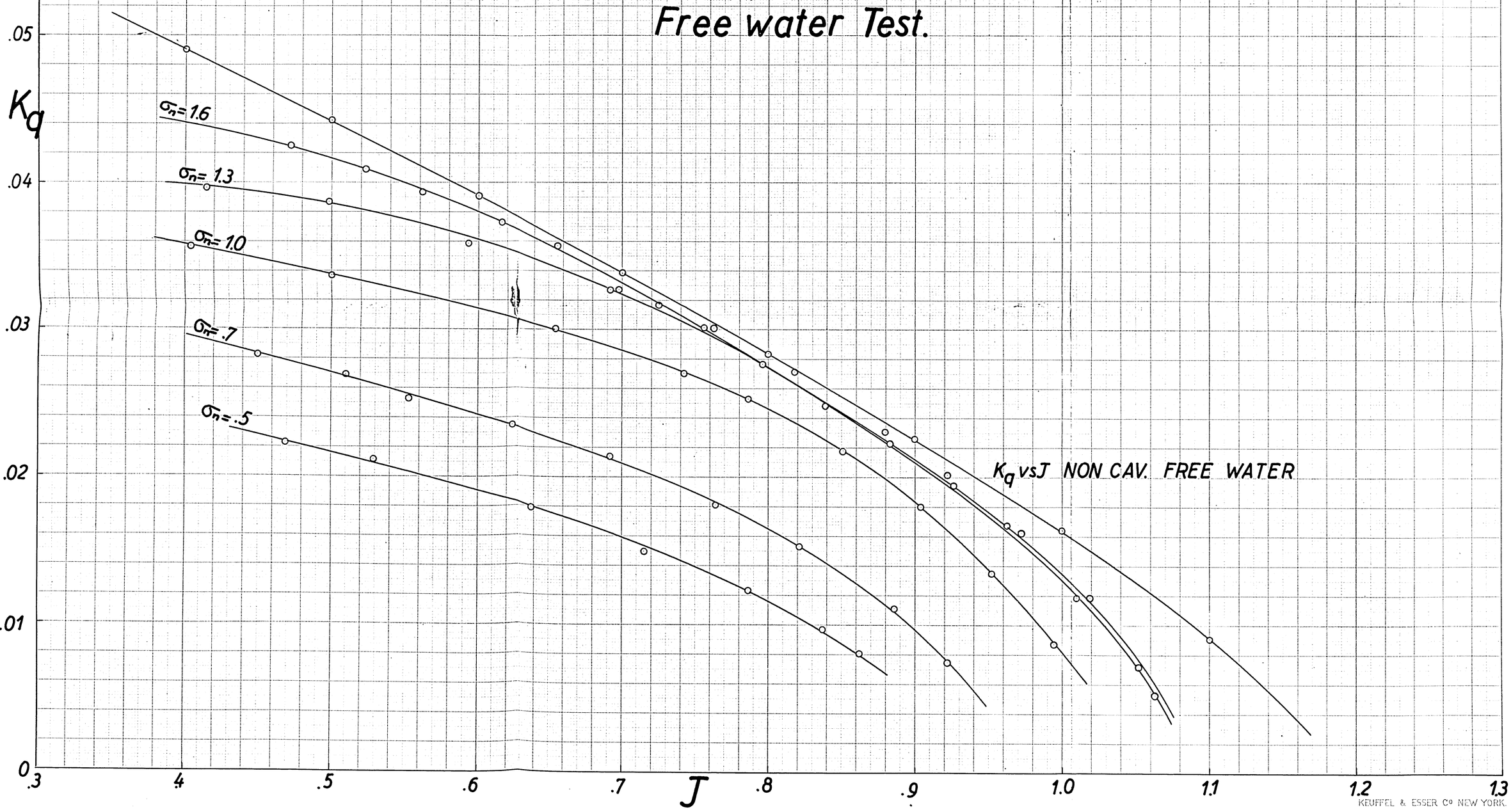

KEUFFEL & ESSER Co NEW YORK.

PLATE 15.

K_t vs. J cavitating.
Screen Test VI.

K_t

$\sigma_n = 1.6$

$\sigma_n = 1.3$

$\sigma_n = 1.0$

$\sigma_n = .7$

$\sigma_n = .5$

H vs. J NON CAV. SCREEN VI.

K_t vs. J NON CAV. SCREEN VI.

J

H m/m

.40 .35 .30 .25 .20 .15 .10 .05 0

.3 .4 .5 .6 .7 .8 .9 1.0 1.1 1.2 1.3

800 700 600 500 400 300 200 100

KEUFFEL & ESSER Co NEW YORK.

PLATE 16.

K_q vs. J cavitating.
Screen Test VI.

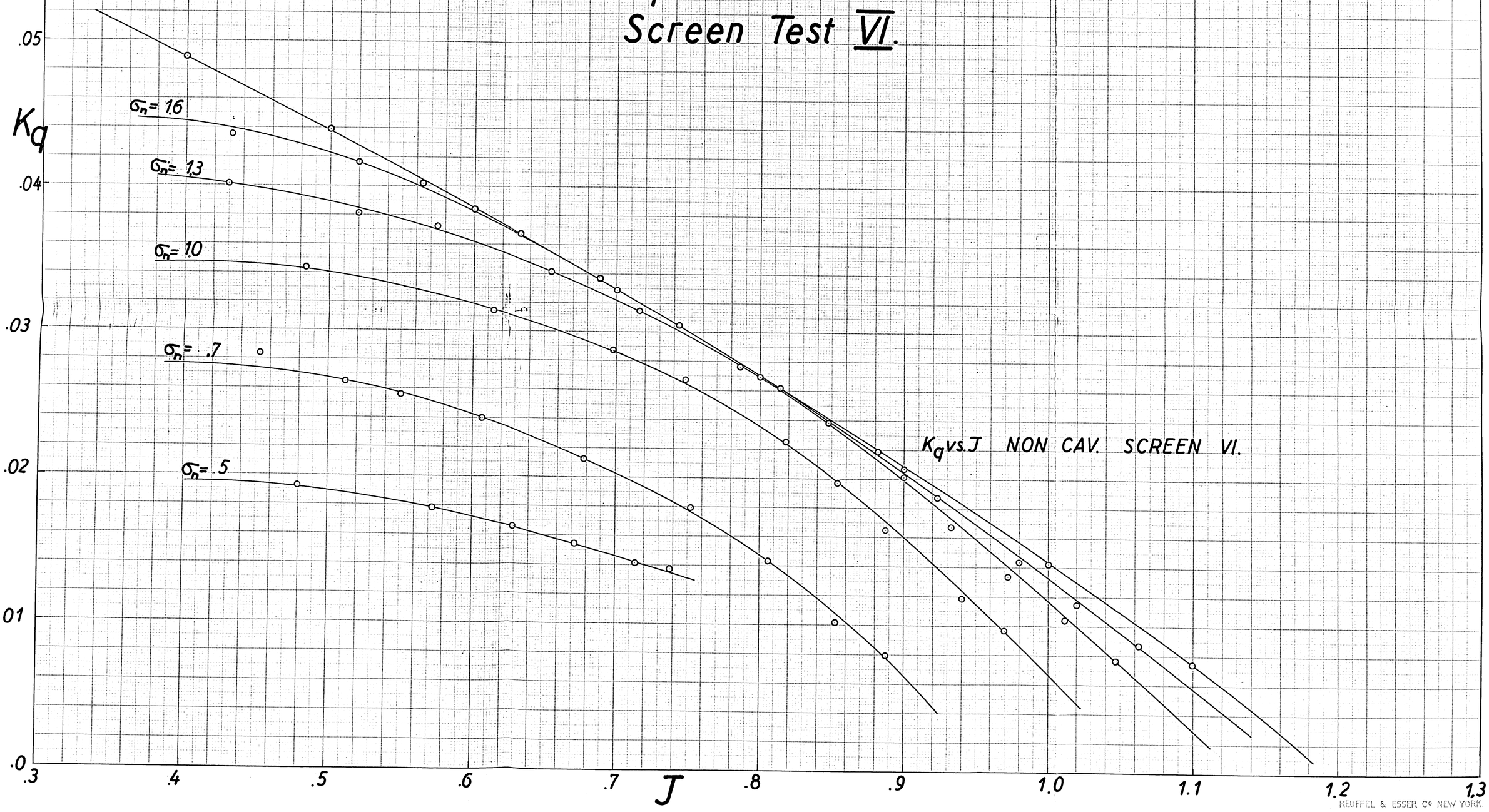

KEUFFEL & ESSER Co NEW YORK.

PLATE 17.

K_t vs. J cavitating.
Screen Test VIII.

K_t

.4 .35 .3 .25 .2 .15 .10 .05 0

$\sigma_n = 1.6$

$\sigma_n = 1.3$

$\sigma_n = 1.0$

$\sigma_n = .7$

$\sigma_n = .5$

.3 .4 .5 .6 .7 J .8 .9 1.0 1.1 1.2 1.3

H vs. J NON CAVITATING
SCREEN VIII.

K_t vs. J NON CAV. SCREEN VIII.

800 700 600 500 400 300 200 100 0

H m/m

PLATE 18.

K_q vs. J cavitating.
Screen Test VIII.

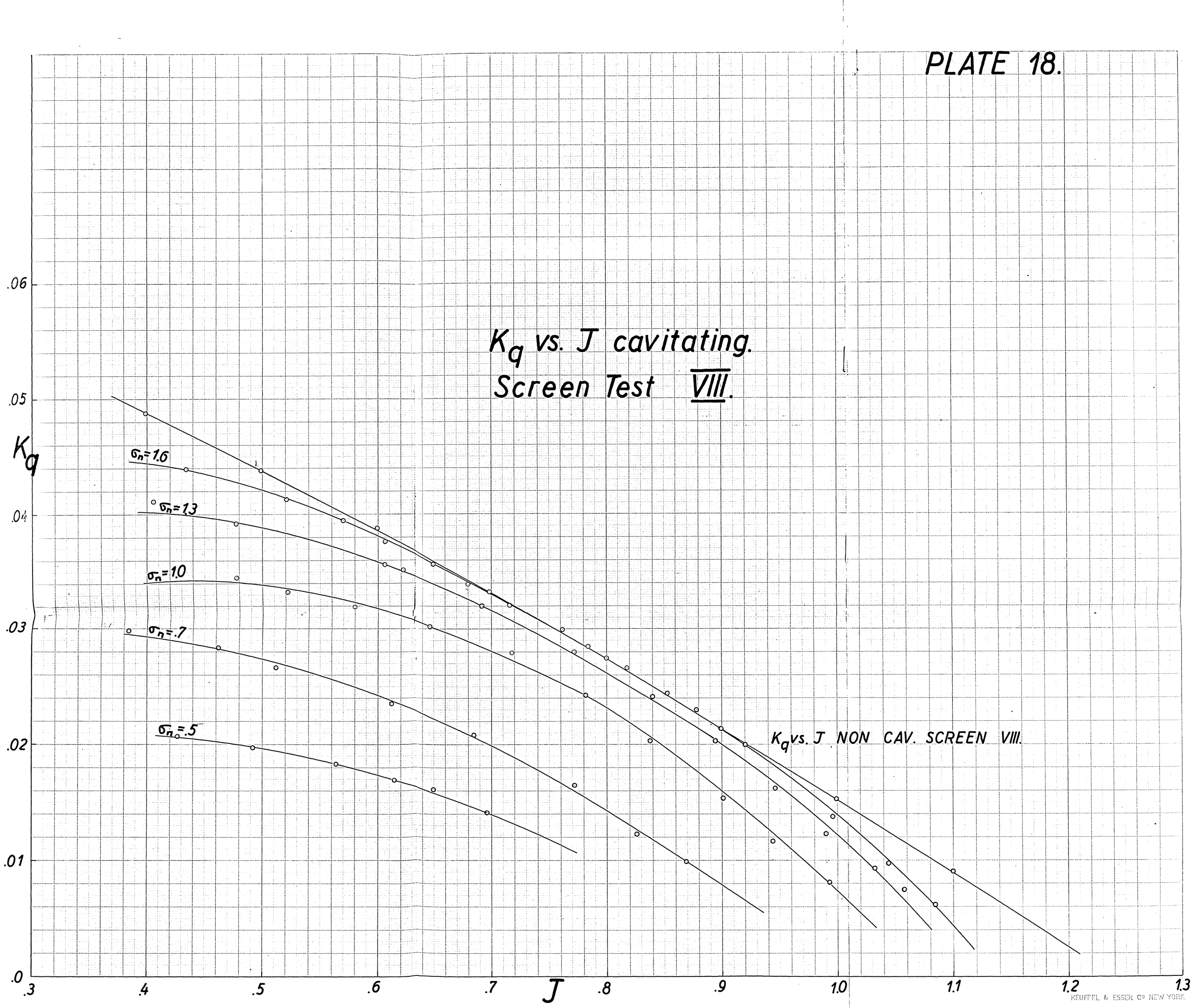

KEUFFEL & ESSER Co NEW YORK